Atmospheric Variability on Luhman 16AB

Elko Gerville-Reache[1,2], Raunak Amanna[1,3], Nima Brivanlou[1,4], Johanna Vos[1,5]
[1] Science Research Mentorship Program,[2] School of the Future [3] Brooklyn Technical High School, [4] Lycée Français de New York, [5] American Museum of Natural History

Abstract:
Brown dwarfs are objects that form in the same way as stars but don't have enough mass to sustain hydrogen fusion; they start off at a high temperature and cool over time. The cooler temperatures allow condensate clouds to form in their atmospheres. Luhman 16AB is a binary brown dwarf system located 6.5 light years away making it the closest and brightest brown dwarf system. We observed Luhman 16AB over 2 nights in the i' and z' bands using the MPG/GROND instrument and extracted their light curves using PSF-fitting. We note Luhman 16B is highly variable while Luhman 16A is not significantly variable above the noise. We measured variability amplitudes of 10.07% and 15.07% for nights one and two respectively. We measured a rotation period of 5.45 hours. We observed phase shifts between the i' and z' bands. Our results suggest a rapidly evolving atmosphere containing multiple cloud layers.

1. INTRODUCTION

Brown dwarfs are objects that have masses in between stars and planets (>80 M_{jup}). They are formed in the same way stars are but don't gain the required mass to sustain hydrogen fusion like stars (Kulkarni et al. (1997)). Stars and brown dwarfs form in large areas of gas known as stellar nurseries. Brown dwarfs peak in the infrared part of the spectrum, meaning it is hard to observe them in optical wavelengths (light humans see in). Although initially hot, they cool off over time having no fuel source. The cooler temperatures of brown dwarfs allow condensates such as molten iron and magnesium silicates to form. These condensates build up over time to form clouds.

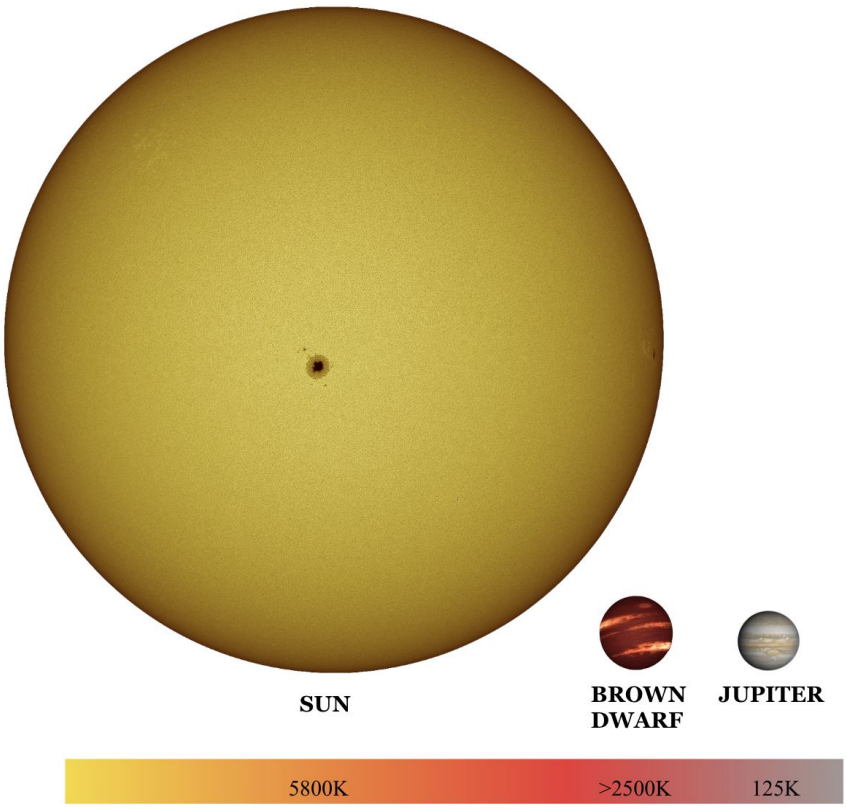

Figure 1: Relative sizes of the Sun, a brown dwarf and jupiter. Brown dwarfs fill the gap between stars and planets in terms of mass and temperature

The atmospheres of brown dwarfs can be used as close analogs for exoplanets, as they have similar atmospheric composition, temperature, and size (~1 R_{jup}) Additionally, these brown dwarfs are easier to observe, as many do not have a bright host star interfering with the observation.

The best way to observe the atmosphere of an object is through direct imaging. Direct imaging is a method of observation, consisting of taking a direct image of the object being observed. Direct imaging for exoplanets is incredibly difficult. Out of the nearly 4000 discovered exoplanets, only 20 have been directly imaged. Furthermore, when exoplanets are directly imaged, the images are not often clear, as their host star causes interference with the observation. However, most brown dwarfs do not orbit a star as they are often free-floating. This lack of adjacent light makes for clearer observations, allowing us to better understand their atmospheres. It is for this reason that brown dwarfs make for the best analogs for exoplanets and their atmospheres.

The L and T spectral classes are two particularly interesting phases of brown dwarf evolution. L dwarfs range from 2300K to 1500K and are characterized by condensates in their atmospheres such as molten iron and silicates which condense and form clouds (Gillon et al. 2013). Cooler than L dwarfs are T spectral types. These dwarfs are characterized by having no cloud cover in their atmospheres and cooler temperatures (<1200K). The transition between L and T spectral types, known as the L/T transition happens over a surprisingly narrow temperature range of 200K and is characterized by dramatic changes in observed properties. L dwarfs go from a reddish color with clouds to a magenta/blue T dwarf with no clouds. At this transition, we will see patchy cloud cover, as they are in the process of breaking up. Additionally, brown dwarfs have fast rotation rates. From their birth, brown dwarfs continually contract and therefore speed up (for approximately 200 million years) to conserve angular momentum. The typical field dwarf has an average rotation period of 3-10 hours.

The rapid rotation combined with weather patterns, consisting of patchy clouds, of L/T dwarfs causes fluctuations in luminosity, called photometric variability. As the brown dwarf rotates, clouds dipping in and out of view will cause the brightness of it to change over time. An example of these weather patterns would be similar to Jupiter's red spot. Monitoring these changes in brightness over time on a flux versus time graph, also known as a light curve allows us to observe an object's variability and subsequently track its weather patterns.

Luhman 16AB (WISE 1049−5319) (Luhman et al. 2013) is a binary brown dwarf system, meaning two brown dwarfs (Luhman 16A and Luhman 16B) rotate around each other. It is located 6.5 light years away from us, making it the third closest system to Earth after the Centauri system and Barnard's star. This pair of brown dwarfs are the closest and brightest brown dwarfs to Earth, meaning they allow for a level of highly detailed measurements and analysis not possible on fainter, further brown dwarfs (Luhman et al. 2013). Luhman 16A is an L7 spectral type, while Luhman 16B is a T0.5 spectral type, placing both objects in the L/T transition.

Additionally, Gillon et al.2013 was the first to discover possible variability in Luhman 16AB. They observed Luhman 16AB for 12 days and classified them in the L/T transition. The paper found a variability amplitude of around 11%, and attributed it to rapidly evolving weather patterns. Biller B. A., et al., 2013, was the first to resolve variability monitoring of both the T0.5 and L7.5. They observed Luhman 16AB for 4 hour periods for 2 days. They observed the r'i'z' JHK bands, and found the r' and i' to be anti correlated with the z' band.

2. OBSERVATIONS

The MPG/ESO 2.2 meter f/8 telescope was used to observe Luhman 16AB. Located at La Silla, Chile, the MPG/ESO telescope is equipped with the GROND (Gamma-Ray Burst Optical/Near-Infrared Detector) instrument, which allows imaging in Sloan g', r', i', z', and near-infrared J, H, K bands. The g' - z' bands allow observations in the 464 nm - 900 nm, or in the optical while the J - K bands offer observations from 1220 to 2090 nm or in the near-infrared part of the spectrum. In the i' and z' band images, Luhman 16AB could be resolved, and we extracted their light curves using PSF photometry (see section 3).

The first observation, carried out on the 24th of February, 2014, was conducted for 6 hours, 24 minutes, and 6 seconds. The second observation, carried out the 25th of February, 2014, lasted 7 hours and 4 seconds. Both nights had a total of 106 light frames, each exposed for 114.9075 seconds, or approximately 115 seconds per observation.

3. DATA REDUCTION

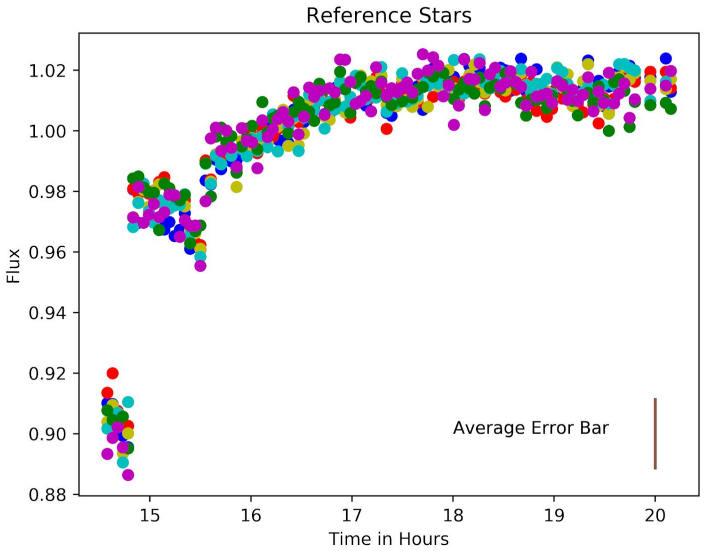

Figure 2: Plot of all reference stars. Since the light curves all follow the same trend, it can be assumed that the reference stars all were affected the same way.

For the data reduction, we used the coding language Python. We created a PSF (Point Spread Function) program to create light curves. The Point Spread Function measures how much a source is blurred out and generates the shape of the blurring. PSF fitting photometry is used when the target star or object has intruding neighboring stars which are too close for standard aperture photometry to be used. PSF fitting photometry models the PSF of the source or target. Stars are point sources, meaning they are too far to resolve and are often blurred due to the atmosphere. PSF fitting

was applied to both Luhman 16AB as well as reference stars to create light curves for every source in the field of view. This is important as reference stars act as a control. Assuming they are not variable, all variations in the raw reference stars' light curve, as seen in *figure 2* must be caused by atmospheric fluctuations on Earth, air mass as well as telescope systematics.

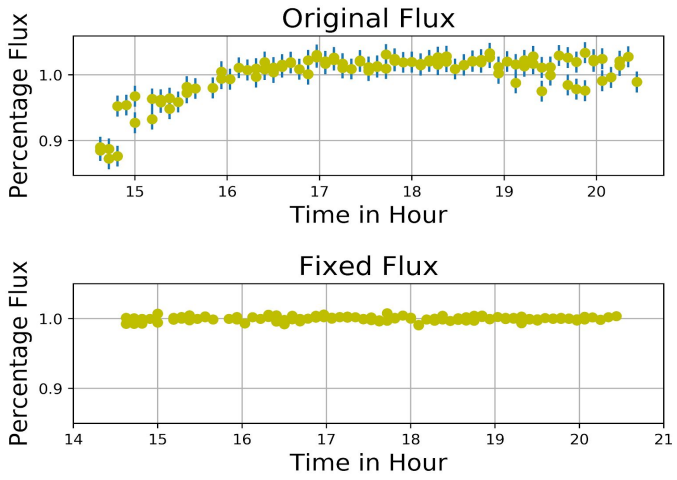

Figure 3: Comparison of the original flux of a reference star and its corrected light curve. The flat trend shows our method is successful.

The reference stars were median combined to create a calibration light curve. This represents the common trend that every star in the image experiences. *Figure 2* demonstrates how each reference star in the image followed the same trend, meaning that we can assume they were all affected by atmospheric conditions the same way. Next, every light source was divided by the calibration curve to divide out the common trend which gives us relatively flat corrected reference stars (*figure 3)* as well as corrected light curves of Luhman 16AB (*figure 4 and 5*). *Figure 3* illustrates the change between the raw reference star curve and the corrected flat curve. All referenced stars seem relatively flat, meaning we think our method worked successfully.

With these now corrected light curves, we were able to more easily understand and determine patterns in the Luhman 16 AB system. We then measured the RMS (root-mean square), which is the noise of each light curve. We used the equation $\frac{stdev(f_{i+1} - f_i)}{\sqrt{2}}$ (f_i = raw, light curve. f_{i+1} = shifted light curve) from Radigan et al. 2014.

4. RESULTS

4.1 *Variability Amplitudes*

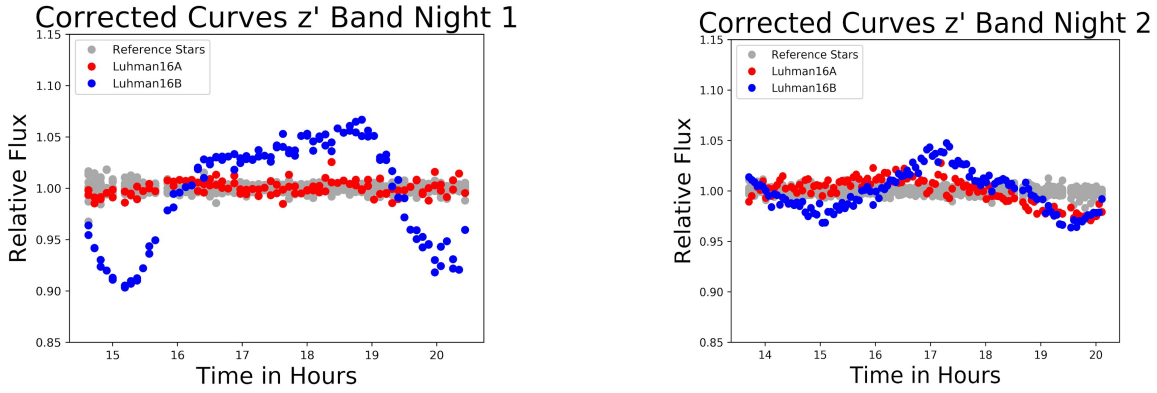

Figures 4 and 5: Corrected light curves from both nights. The light curve from Luhman 16B changes drastically from night to night pointing to fast light curve evolution.

Figures 4 and 5 show the corrected light curves of Luhman 16 A and B. We compared the relative fluxes of Luhman 16AB to the relative fluxes of the reference stars. As expected the reference stars did not have a significant change in flux (illustrated by the flat light curve). As shown in the graph Luhman 16B has a large change in flux over time. On the other hand, the flux of Luhman 16A does not change as much as Luhman 16B. Since Luhman 16A is not variable above the noise, we focused on Luhman 16B for this study.

	Our N1	Our N2	Biller 2013
i'	10.07%	15.07%	6%
z'	16.35%	8.38%	7%

Figure 6: Table of amplitude values for Luhman 16B. Both nights of data are compared to the amplitude values of Biller et al. (2013).

The amplitude of Luhman 16B changed rapidly from night to night. This strong variability is indicative of evolving weather patterns or moving cloud structures and studying this change represents observing weather patterns. As shown in figure 6 both the i' and z' bands drastically change from the first night to the next. The i' band increases by around 5%, while the z' band decreased by around 8%. This depicts the incredible speed of the changing weather patterns. In a matter of a couple hours the surface can have a completely different cloud cover. However, in the Biller paper only 1% change was observed. This may due to the weather on earth or technology available at the time. Apai et al. 2017 have observed variability of Luhman 16B to evolve rapidly

4.2 *Phase Shifts*

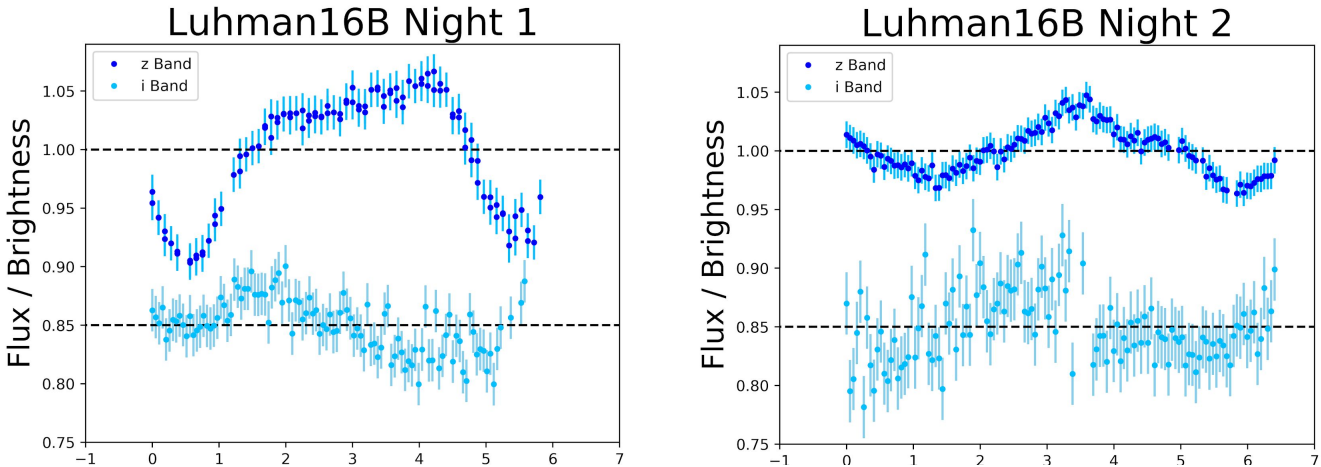

Figures 7 and 8 show simultaneous i' and z' light curves of Luhman 16B for both nights of observations. During the first night, the i' and z' bands are out of phase with each other around the 1 to 5-hour mark. This is characterized by the light curves of each band moving antiparallel with each other; as the z' band increases in flux, the i' band independently decreases. The bands in Night 1 show a continuous change in flux over time. The change does not seem to be following a pattern and more a random change. Due to atmospheric conditions as well as clouds affecting the visibility of night 2, the i' band does not follow a clear trend. In addition, there are many outliers to the i' band in night 2, making it more inconclusive. These factors cause the light curve to be a lot less clear, making it more challenging to discern between in phase and out of phase. However, overall it seems like night 2 follows an in-phase trend. The out of phase light curves during night 1 supports the findings of Biller et al. (2013), where the i' and z' bands also followed an anticorrelated trend. Biller et al. (2013) reported that the r' and

Figures 7 and 8: Phase diagrams of both i' and z' bands across the two nights. The i' and z' band follow an anti-correlated (out of phase) trend.

i' bands are anticorrelated with the z' band.

4.3 *the Rotational Period of Luhman 16B*

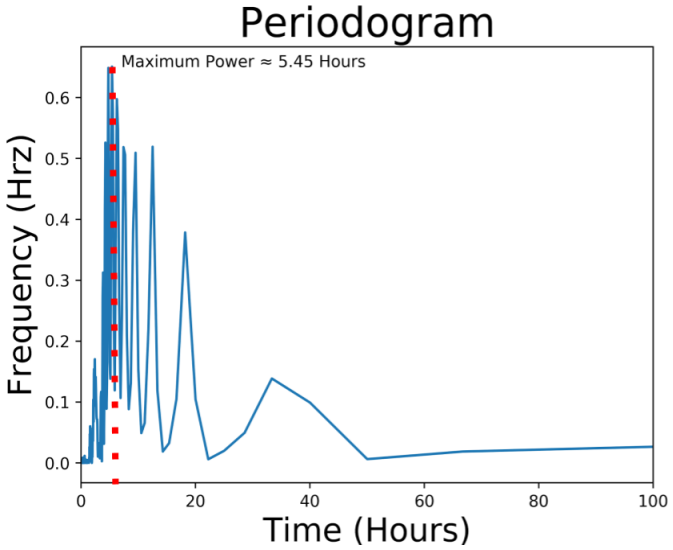

This Work	5.45 h
Biller 2013	>3.5 h
Gillon 2013	4.87 +-0.1 h

Figures 9 and 10: This periodogram and table depicts the rotation period, or the time it takes to complete one revolution, of Luhman 16B

Using the Lomb-Scargle method, we found that the period of rotation for Luhman 16B was 5.45 hours. We use the Lomb-Scargle method, which is a way to produce the power spectrum of our observation. The power spectrum shows the likelihood of each rotation period, with the peak being the most likely, which in our case is 5.45 hours. This is similar to the rotation period found in Biller et al. (2013) and Gillion et al. (2013).

5. DISCUSSION

5.1 *Phase*

Night one demonstrated clear out of phase characteristics while night two followed more of an in-phase trend. This fast evolution of phase across the two nights demonstrates how rapidly evolving the atmospheric structures of Luhman 16B are. This points to rapidly evolving weather patterns at different levels in the atmosphere. Biller et al. 2013 asserts that the z' band probes a brown dwarf's atmosphere deeper than the i' band due to varying opacities in the atmosphere blocking certain bands. Thus, when the i' and z' bands are out of phase as depicted in *figure 11*, it suggests that there are different cloud layers at different altitudes, or more literally, weather patterns differ greatly from each other at different levels in the atmosphere. For example, on Earth, cirrus clouds form higher up in the atmosphere, whereas cumulus clouds from lower in the atmosphere. These phase observations allow for probing and monitoring of weather patterns in Luhman 16B across different levels.

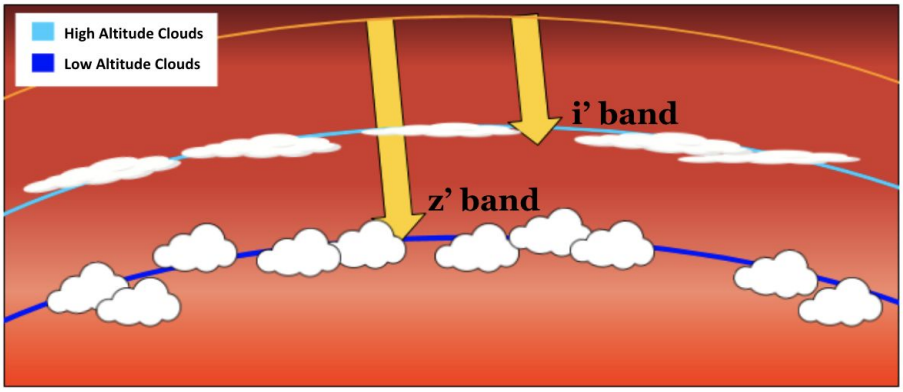

Figure 11: Atmosphere diagram of Luhman 16B depicting how different bands probe different levels of the atmosphere. Studying these bands allows us to monitor weather patterns on Luhman 16B across varying atmosphere levels.

5.2 *Period*

When considering other rotation period measurements (Biller et al. 2013, Gillon et al. 2013) of Luhman 16AB, we see similar results. For example, Biller et al. 2013 found a period of rotation of >3.5 hours, and Gillon et al. 2013 found a period of rotation of 4.87 +/-0.1 hours. This difference in observation is due to the difference in the precision of the observation in Biller et al. (2013). Biller et al. (2013), who concluded a >3.5 hour period of observation, observed for 4 hours over the course of one night. Gillon et al. (2013), who concluded a 4.87 +-.1 hour period of rotation had observed for 12 nights. Our observation which took place over the course of two nights found a period of rotation of 5.45 hours. While Gillon et al. (2013) used the TRAPPIST (Transiting Planets and Planetesimals Small Telescope) to observe the i' and z' bands, our observations with the GROND instrument, which allowed us to gain better

resolution in our observation. Gillon et al. (2013) used aperture photometry to resolve both Luhman A and B as one object, as they could not separate them, whereas we use point spread function (PSF) to resolve both components. Additionally, while uses the same instrument and wavelengths bands as we do, they only observe for one night, whereas we observe for two.

6. NEXT STEPS

6.1 *Multi-Wavelength GROND Data*

The Gamma-ray Burst Optical/Near Infrared Detector (GROND) camera captures data in 7 bands, allowing observations in g', r', i', z', J, H, and K bands. In this study only the i' and z' bands were used, therefore there are a potential 5 more bands to study for more data and light curves. The i' and z' bands were used as they are in the optical range of the spectrum. Although brown dwarfs are brightest in the infrared, because Luhman 16AB is so close to Earth, we were able to look at it in the optical spectrum. This is significant because as the wavelength increases, the resolution of the data decreases meaning bands in the optical will be able to resolve both Luhman 16 A and B while bands in the infrared won't. This would result in Luhman 16AB appearing as a singular object, preventing photometric observations on each individual brown dwarf. Because of time constraints as well as the decreased resolution, the other 5 bands were not used, however examining all the data could give more insight on weather patterns throughout Luhman 16B's atmosphere.

6.2 *Monitoring Exoplanets with the James Webb Space Telescope*

The launch of the James Webb Space Telescope will allow far more detailed observations in the infrared. Use of the JWST will allow us to better understand the atmospheres of exoplanets, as its capability to directly image planets will grant us unprecedented data and access into their atmospheres. The processes and discoveries already made regarding the atmospheres of brown dwarfs will be important when it comes to studying the atmospheres of exoplanets. This is because brown dwarfs, having similar composition, size, and most importantly temperature as exoplanets, make for fantastic analogs for exoplanets.

6.3 *Long-Term Observations with the Transition Exoplanet Survey Satellite (TESS)*

Luhman 16AB was recently observed with the Transiting Exoplanet Survey Satellite better known as TESS. This satellite is designed to detect transiting exoplanets. The transit method measures the change in brightness of stars when planets cross in front of them along our line of sight. TESS's area of observation is 400 times larger than that covered by the Kepler mission. During its 2 year mission, it is predicted to discover around 20,000 exoplanets. However, its observations are also ideal for brown dwarf variability searches in the optical. Each TESS sector is observed continuously for around 30 days. This will allow us to observe Luhman 16AB for nearly 150 rotations. We can use TESS to observe the change in brightness of Luhman 16AB to learn more about their variability and clouds.

7. REFERENCES

Biller B. A., et al., 2013, The Astrophysical Journal, 778, L10
Gillon M., et al., 2013, A&A, 555, L5
Luhman K. L., 2013, ApJ, 767, L1
Radigan J., Lafrenière D., Jayawardhana R., Artigau E., 2014, ApJ, 793, 75